
Federated Sparse Training: Lottery Aware Model Compression for Resource Constrained Edge

Anonymous Author(s)

Affiliation

Address

email

Abstract

1 Limited computation and communication capabilities of clients pose significant
2 challenges in federated learning (FL) over resource-limited edge nodes. A poten-
3 tial solution to this problem is to deploy off-the-shelf sparse learning algorithms
4 that train a binary sparse mask on each client with the expectation of training
5 a consistent sparse server mask. However, as we investigate in this paper, such
6 naive deployments result in a significant accuracy drop compared to FL with dense
7 models, especially under clients' low resource budgets. In particular, our investiga-
8 tions reveal a serious lack of consensus among the trained masks on clients, which
9 prevents convergence on the server mask and potentially leads to a substantial drop
10 in model performance. Based on such key observations, we propose *federated*
11 *lottery aware sparsity hunting* (FLASH), a unified sparse learning framework to
12 make the server win a lottery in terms of a sparse sub-model, which can greatly
13 improve performance under highly resource-limited client settings. Moreover, to
14 address the issue of device heterogeneity, we leverage our findings to propose
15 *hetero-FLASH*, where clients can have different target sparsity budgets based on
16 their device resource limits. Extensive experimental evaluations with multiple
17 models on various datasets (both IID and non-IID) show superiority of our models
18 in yielding up to $\sim 10.1\%$ improved accuracy with $\sim 10.26\times$ fewer communication
19 costs, compared to existing alternatives, at similar hyperparameter settings.

20 1 Introduction

21 Federated learning (FL) [30] is a popular form of distributed training, which allows multiple clients
22 to learn a shared global model without the requirement to transfer their private data. However, clients'
23 heterogeneity and resource limitations pose significant challenges for FL deployment over edge
24 nodes, including mobile phones and IoT devices. To resolve these issues, various methods have
25 been proposed over the past few years including efficient learning for heterogeneous collaborative
26 training [27, 42], distillation [12], federated dropout techniques [15, 4], efficient aggregation for
27 faster convergence and reduced communication [34, 25]. However, these methods do not necessarily
28 address the growing concerns of highly computation and communication limited edge.

29 Meanwhile, reducing the memory, compute, and latency costs for deep neural networks in centralized
30 training is an active area of research. In particular, recently proposed *sparse learning* strategies
31 [8, 20, 31, 5, 33] effectively train weights and associated binary *sparse masks* to allow only a fraction
32 of model parameters to be updated during training, potentially enabling the lucrative reduction in
33 both the training time and FLOPs [32, 33], while creating a *model to meet a target parameter density*
34 *denoted as d , and is able to yield accuracy close to that of the unpruned baseline.*

35 However, the challenges and opportunities of sparse learning in FL is yet to be fully unveiled. Only
36 very recently, few works [2, 16] have tried to leverage sparse learning in FL primarily to show their
37 efficacy in non-IID settings. Nevertheless, these works primarily used sparsity for non-aggressive

38 model compression, limiting the actual benefits of sparse learning, and assumed multiple local epochs,
 39 that may further increase the training time for stragglers making the overall FL process inefficient [40].
 40 Moreover, the server-side pruning used in these
 41 methods may not necessarily adhere to the layers’ pruning sensitivity¹ [7] that often plays
 42 a crucial role in sparse model performance [20, 39, 35]. Another recent work, ZeroFL [32],
 43 has explored deploying sparse learning in FL settings with limited client epochs. However, [32]
 44 could not leverage any advantage of model sparsity in the clients’ down-link communication cost
 45 and had to keep significantly more parameters active compared to a target d to yield good
 46 accuracy. Moreover, as shown in Fig. 1(b), for $d = 0.05$, ZeroFL still suffers from substantial
 47 accuracy drop of $\sim 14\%$ compared to the baseline.

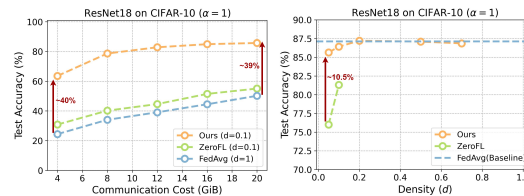


Figure 1: Comparison of (a) accuracy at different communication budget with, ZeroFL [32] and FedAvg. (w/ $d = 1.0$) (b) Accuracy vs. parameter density of each client. Proposed approach can significantly outperform the existing alternative [32] at ultra-low target parameter density (d).

55 **Our Contributions.** Our contribution is fourfold. In view of the above limitations, we first identify
 56 crucial differences between a centralized and the corresponding FL model, in learning the sparse
 57 masks for each layer. In particular, we observe that in FL, the server model fails to yield convergent
 58 sparse masks. In contrast, the centralized model show significantly higher convergence trend in learning
 59 sparse masks for all layers. We then experimentally demonstrate the utility of pruning sensitivity
 60 and mask convergence in yielding good accuracy setting the platform to close the performance gap in
 61 sparse FL.

62 We then leverage our findings and present *federated lottery aware sparsity hunting* (FLASH), a
 63 sparse FL methodology addressing the aforementioned limitations. At the core, FLASH leverages
 64 a two-stage FL, a robust and low-cost layer sensitivity evaluation stage which identifies a good
 65 predefined sparse mask for the clients and a training stage. We claim the first stage to play a key role
 66 in communication-efficient learning of a model which yields SOTA accuracy in sparse FL.

67 To deal with resource heterogeneity, we further extend our methodologies to *hetero*-FLASH, where
 68 we assume a critical scenario of individual clients having different d . Here, to deal with the unique
 69 problem of the server selecting different sparse models for clients, we present server-side gradual
 70 mask sub-sampling, that identifies sparse masks via a form of layer sensitivity re-calibration, starting
 71 for models with highest to that with lowest density support.

72 We conduct extensive experiments on MNIST, FEMNIST, and CIFAR-10 with different models
 73 for both IID and non-IID client data partitioning. Experimental results show that, compared to the
 74 existing alternative [32], at iso-hyperparameter settings, FLASH can yield up to $\sim 8.9\%$ and $\sim 10.1\%$,
 75 on IID and non-IID data distribution of CIFAR-10 dataset, respectively, with reduced communication
 76 of up to $\sim 10.2\times$ (Table 3).

77 2 Related Works

78 **Model Pruning.** Over the past few years, a plethora of research has been done to perform efficient
 79 model compression via pruning, particularly in centralized training [29, 9, 28, 38, 14]. Pruning
 80 essentially identifies and removes the unimportant parameters to yield compute-efficient inference
 81 models. More recently, sparse learning [8, 20, 5, 33], a popular form of model pruning, has gained
 82 significant traction due to its popularity in yielding FLOPs advantage and potential speed-up even
 83 during training. In particular, it ensures only $d\%$ of the model parameters remain non-zero during the
 84 training for a target parameter density d , potentially enabling training complexity reduction.

85 **Dynamic network rewiring (DNR).** We leverage DNR [20], to learn the sparsity mask of each
 86 client. In DNR, a model starts with randomly initiated mask following the target parameter density d .
 87 After an epoch, the client evenly prunes the lowest $p_r\%$ weights from each layer based on absolute
 88 magnitude, where p_r is prune rate. Note, this $p_r\%$ pruning happens on top of the sparse model
 89 with density d , allowing $p_r\%$ weights to be regrown. DNR then ranks each layer based on the
 90 normalized contribution of the summed non-zero weight magnitudes. Finally, the client regrows total
 91 $p_r\%$ weights in a non-uniform way, allowing more regrowth to the layers having higher rank. This

¹A layer with higher sensitivity demands higher % of non-zero weights compared to a less sensitive layer.

92 process iteratively repeats over epochs to finally learn the mask. **Federated learning for resource**
 93 **and communication limited edge.** To address device heterogeneity, existing works have explored
 94 the idea of heterogeneous training [15, 6, 37] allowing different clients to train on different fractions
 95 of full-model based on their compute-budget. On a parallel track, various optimizations are proposed
 96 in FL training framework to yield faster convergence, thus requiring fewer communication rounds
 97 [11, 10, 41, 26, 34, 17, 1].

98 A few research have leveraged pruning in FL [23, 18, 24]. In particular, in LotteryFL [23] and
 99 PruneFL [18], clients need to send the full model to the server regularly costing bandwidth. Moreover,
 100 in [23], each client trains a personalized mask to maximize the performance only on the local data.

101 Only a few contemporary works [16, 2, 32] tried to leverage the benefits of sparse learning in
 102 federated settings. In particular, [16] relied on a randomly initialized sparse mask, and recommended
 103 keeping it frozen [21] throughout the training, yet failed to provide any supporting intuition. FedDST
 104 [2], on the other hand, leveraged the idea of RigL [8] to perform sparse learning of the clients and
 105 relied on magnitude pruning at the server-side that does not necessarily adhere to the layer sensitivity
 106 towards a target density. Moreover, both the approaches assumed all clients can support a fixed d , a
 107 large number of local epochs, and focused primarily on only highly non-IID data without targeting
 108 ultra-low density d . More importantly, neither of these works investigated the key differences between
 109 centralized and FL sparse learning. With similar philosophy as ours, ZeroFL [32] first identified
 110 a key aspect of sparse learning in FL in terms of all clients’ masks to be within 30% of the total
 111 model weights to yield good accuracy at high compression. However, ZeroFL suffered significantly
 112 in failing to exploit a proportional advantage in communication saving as even for low parameter
 113 density d , all clients had to download the dense model and send back at least a model with $d = 0.3$.
 114 Furthermore, these algorithms sacrifice significant accuracy at ultra-low d .

115 3 Revisiting Sparse Learning: Why Does it Miss the Mark in FL?

116 Sparse learning uses proxies, including normalized momentum and normalized values of the non-zero
 117 weights [20, 5], to decide the layers and weights that are more sensitive towards pruning and update
 118 the binary sparse mask accordingly. Note, centralized training has shown significant benefits with
 119 sparse learning with FLOPs reduction during forward operations [8], and potential training speed-up
 120 of up to $3.3\times$ [32] while maintaining close to the baseline accuracy, even at $d \leq 0.1$. We now use a
 121 sparse learning, namely [20], in FL settings (refer to Table 1 for details) on CIFAR-10, where each
 122 client separately performs [20] to train a sparse ResNet18 and meet a fixed parameter density d ,
 123 starting from a random sparse mask. After sending the updates to server, it aggregates them using
 124 FedAvg. We term this as *naive sparse training* (NST).

Table 1: FL training settings considered in this work.

Dataset	Model	#Params.	Data-partitioning	Rounds (T)	Clients (C_N)	Clients/Round (c_r, c_d)	Optimizer	Aggregation type	#Local epochs (E)	Sensitivity warmup (E_d)	Batch Size
MNIST	MNISTNet	262K	LDA	400	100	10, 10	SGD	FedAvg [30]	1	10	32
CIFAR-10	ResNet18	11.2M		600							16
FEMNIST	Same as [3]	6.6M	[34]	1000	3400	34, 34					

125 **Observation 1.** *At high compression $d \leq 0.1$, the collaboratively learned FL model significantly*
 126 *sacrifices performance, while the centralized sparse learning yields close to baseline performance.*

127 As shown in Fig.2(a), naive deployment of sparse learning significantly sacrifices accuracy in FL.
 128 In particular, for $d = 0.1$, the trained server-side model suffers an accuracy drop of 3.67%. At
 129 even lower $d = 0.05$, this drop significantly increases to 12.03%, hinting at serious limitations of
 130 sparse learning in FL. However, in centralized sparse learning, the model yields close to the baseline
 131 accuracy, even at $d = 0.05$.

132 **Observation 2.** *As the training progresses, the sparse masks in centralized training tend to agree*
 133 *across epochs, showing convergence, while server mask in FL does lack agreement across rounds.*

134 **Definition 1. Sparse mask mismatch.** For a model at round t , we define the *sparse mask mismatch*
 135 (SM) sm^t as the Jaccard distance that is measured as follows.

$$sm^t = 1 - \frac{(\sum_{l=1}^L \mathcal{M}_l^t \cap \mathcal{M}_l^{t-1})}{(\sum_{l=1}^L \mathcal{M}_l^t \cup \mathcal{M}_l^{t-1})} \quad (1)$$

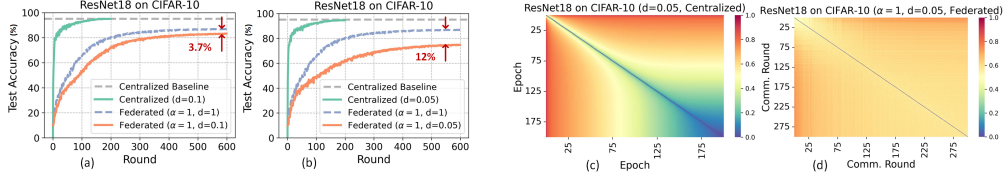


Figure 2: (a-b) Accuracy vs. round plot on deployment of off-the-shelf [20] sparse learning in FL for different d , (c-d) visualization of the Model’s SM in terms of Jaccard distance while training with sparse learning for (c) centralized and (d) FL, respectively.

136 where \mathcal{M}_l^t represents the sparse mask tensor for layer l at the end of round t . Interestingly, as depicted
 137 in Fig. 2(a), the SM for centralized learning tends to zero as the training progresses. In contrast,
 138 with the same model, dataset and d values, in FL, the SM remains > 0.4 indicating a substantial
 139 distinction in the sparse mask learning between centralized and federated learning.

140 4 FLASH: Methodology

141 To win a lottery of having a sparse network yielding high accuracy at reduced parameters, we identify
 142 a key characteristic of sparse learning, the pruning sensitivity. To explicitly adhere to this important
 143 aspect, in FLASH, we present a two-stage sparse FL method, **stage1**: targeting sensitivity analysis to
 144 identify good initial sparse mask for each layer, **stage2**: targeting training to weights. In particular,
 145 to evaluate layer sensitivity in stage1, the server randomly selects a small fraction of clients (\mathcal{C}_d),
 146 each locally sparse learning [20] for few warm-up epochs (E_d) ($L4-8$ in Algo. 1). Upon collection of
 147 layer-wise sensitivity from the clients, for each layer l , the server calculates the average sensitivity
 148 per layer² \hat{d}^l as $\frac{\sum_{i=1}^{c_d} d_i^l}{c_d}$, where d_i^l is the density at layer l in i^{th} client. As these averaged layer-wise
 149 density values may not necessarily yield to the target density d , for a model with K parameters we
 150 follow the following *density re-calibration*

$$d_c^l = \hat{d}^l \cdot r_f, \text{ where } r_f = \frac{d \times K}{\sum_{l=1}^L \hat{d}^l \cdot k^l} \quad (2)$$

151 k^l is dense model’s parameter size for layer l . For each layer l of the model, the server then creates a
 152 binary sparse mask tensor that is randomly initialized, with a fraction of 1s $\propto d_c^l$ ($L9$). In stage2, at
 153 each round, the clients train the model for E epochs ($L19-24$) with a mask frozen ($L22$).

154 However, in FL settings, the masks often show poor convergence (§3, Obs. 2). To address this, in
 155 stage 2, we present the idea of sparse FL with pre-defined layer masks at initialization ($L13$). The
 156 frozen mask allows all the clients to have a forcefully convergent mask ($sm^t = 0$ for all t). Moreover,
 157 as FLASH disentangles the sensitivity evaluation stage from the training, the pre-defined mask in this
 158 scenario benefits from the notion of layer sensitivity. Interestingly, earlier research [2] hinted at poor
 159 model performance with pre-defined masks, contrasting ours where we see significantly improved
 160 model performance, implying the importance of stage1 (as will be elaborated in §5).

161 **Extension to support heterogeneous parameter density.** To support different density budgets
 162 for different clients, we now present hetero-FLASH. Let us assume a total of N support densities
 163 $d_{set} = [d_1, \dots, d_M]$, where $d_i < d_{i+1}$. First, we perform a sensitivity warm-up, to create the masks for
 164 the clients’ with the highest density d_N . For any other density d_i , a sparse mask is subsampled from
 165 the mask with density d_{i+1} . Note, while creating the mask from d_{i+1} to d_i , we follow the layer-wise
 166 density re-calibration approach as mentioned earlier. In hetero-FLASH, server aggregates the update
 167 following *weighted fedAvg* (WFA) instead of fedAvg. In particular, with similar inspiration as [6], to
 168 give equal importance to each parameter update in such heterogeneous settings, WFA averages the
 169 values by their number of non-zero occurrences among the participating clients.

170 5 Experiments

171 **Datasets and Models.** We evaluated the performance of FLASH on MNIST[22], Federated EMNIST
 172 (FEMNIST) [3], and CIFAR-10 [19] datasets with the CNN models described in [30], [3], and
 173 ResNet18, respectively. For data partitioning of MNIST and CIFAR-10, we use Latent Dirichlet

²For a sparse model it is evaluated as the ratio $\frac{\# \text{ of non-zero layer parameters}}{\# \text{ layer parameters}}$ [7].

Algorithm 1: FLASH Training.

Data: Training rounds T , local epochs E , client set $[C_N]$, clients per rounds c_r , target density d , sensitivity warm-up epochs E_d , density warm up client count c_d , initial value of freeze masks $m_{freeze} = 0$ and aggregation type t_{aggr} .

```

1  $\mathcal{M}^{init} \leftarrow \text{createRandomMask}(d)$ 
2  $\Theta^{init} \leftarrow \text{initMaskedWeight}(\mathcal{M}^{init})$ 
3 serverExecute:
4 Randomly sample  $c_d$  clients  $[C_d] \subset [C_N]$ 
5 for each client  $c \in [C_d]$  in parallel do
6    $\Theta_c \leftarrow \text{clientExecute}(\Theta^{init}, E_d, 0) \# m_{freeze} = 0$ 
7    $S_c \leftarrow \text{computeSensitivity}(\Theta_c)$ 
8 end
9  $\mathcal{M}^0 \leftarrow \text{initMask}([S_c], d)$ 
10  $\Theta^0 \leftarrow \text{initMaskedWeight}(\mathcal{M}^0)$ 
11  $m_{freeze} \leftarrow 1$ 
12 for each round  $t \leftarrow 1$  to  $T$  do
13   Randomly sample  $c_r$  clients  $[C_r] \subset [C_N]$ 
14   for each client  $c \in [C_r]$  in parallel do
15      $\Theta_c^t \leftarrow \text{clientExecute}(\Theta^{t-1}, E, m_{freeze})$ 
16   end
17    $\Theta^t \leftarrow \text{aggrParam}([\Theta_c^t], t_{aggr})$ 
18 end
19 clientExecute $(\Theta_c, E, m_{freeze})$  :
20  $\Theta_{c^0} \leftarrow \Theta_c$ 
21 for local epoch  $i \leftarrow 1$  to  $E$  do
22    $\Theta_{c^i} \leftarrow \text{doSparseLearning}(\Theta_{c^{i-1}}, m_{freeze})$ 
23 end
24 return  $\Theta_{c^E}$ 

```

Table 2: Results with FLASH and its comparison with NST and PDST.

Dataset	Data Distribution	Density (d)	Baseline Acc %	NST Acc %	PDST Acc %	FLASH Acc %
MNIST	IID ($\alpha = 1000$)	1.0	98.79 \pm 0.06	-	-	-
		0.1	-	97.57 \pm 0.11	97.09 \pm 0.18	98.21 \pm 0.06
		0.05	-	95.19 \pm 0.56	94.8 \pm 1.04	97.46 \pm 0.14
	non-IID ($\alpha = 1.0$)	1.0	98.76 \pm 0.06	-	-	-
		0.1	-	97.36 \pm 0.19	96.82 \pm 0.25	97.96 \pm 0.13
		0.05	-	95.75 \pm 0.31	95.34 \pm 0.77	97.3 \pm 0.26
	non-IID ($\alpha = 0.1$)	1.0	98.45 \pm 0.17	-	-	-
		0.1	-	96.19 \pm 0.22	94.41 \pm 1.23	97.22 \pm 0.43
		0.05	-	91.66 \pm 1.74	91.06 \pm 1.1	95.7 \pm 0.37
CIFAR-10	IID ($\alpha = 1000$)	1.0	88.56 \pm 0.06	-	-	-
		0.1	-	84.89 \pm 0.26	86.72 \pm 0.09	88 \pm 0.28
		0.05	-	77.48 \pm 0.54	84.38 \pm 0.12	86.99 \pm 0.14
	non-IID ($\alpha = 1.0$)	1.0	87.13 \pm 0.18	-	-	-
		0.1	-	83.46 \pm 0.19	85.07 \pm 0.24	86.42 \pm 0.49
		0.05	-	75.1 \pm 0.76	83.33 \pm 0.14	85.64 \pm 0.58
	non-IID ($\alpha = 0.1$)	1.0	77.64 \pm 0.49	-	-	-
		0.1	-	71.18 \pm 1.23	74.82 \pm 0.72	76.74 \pm 1.46
		0.05	-	61.29 \pm 2.76	72.32 \pm 1.05	75.47 \pm 2.31
FEMNIST	non-IID	1.0	84.68 \pm 0.20	-	-	-
		0.1	-	76.92 \pm 0.42	76.01 \pm 1.26	82.70 \pm 0.26
		0.05	-	61.9 \pm 2.6	63.65 \pm 0.86	81.18 \pm 0.36

Allocation (LDA)[34] with three different α ($\alpha = 1000$ for IID and $\alpha = 1$ and 0.1 for non-IID). For FEMNIST, we employ the same setting as in [11], which partitions the data based on the writer into 3400 clients, making it inherently non-IID.

Training Hyperparameters. We use Clients’ starting learning rate (η_{init}) as 0.1 that is exponentially decayed to 0.001 (η_{end}) at the end of training. Specifically, learning rate for participants at round t is $\eta_t = \eta_{init} (\exp(\frac{t}{T} \log(\frac{\eta_{init}}{\eta_{end}})))$. In all the sparse learning experiments, prune rate is set to 0.25³. Summary of the rest of the hyperparameters can be found in 1. Furthermore, we report the final results as the averaged accuracy with corresponding std of three different seeds in the tables.

5.1 Experimental Results with FLASH

To understand the importance of stage1 in FLASH methodology, we identify a baseline training with uniform layer sensitivity driven *pre-defined sparse training* (PDST) in FL. Table 2 details the performance of FLASH at different levels of d , for various choices of sparse learning methods. In particular, as we can see in Table 2 column 5 and 6, the performance of both NST and PDST produced models cost heavy accuracy drop at ultra low parameter density $d = 0.05$. For example, on CIFAR-10 ($\alpha = 0.1$), models from NST and PDST sacrifice an accuracy of 16.35% and 5.32%, respectively.

³Prune rate controls the fraction of non-zero weights participating in the redistribution during sparse learning.

Table 3: Comparison of FLASH on various performance metrics with existing alternative sparse federated learning schemes.

Dataset	Data Distribution	Method	Density	Acc%	Down-link Savings	Up-link Savings
CIFAR-10	IID	ZeroFL [32]	0.1	82.71 ± 0.37	1×	1.6×
		FLASH (ours)	0.1	88 ± 0.28	9.8×	9.8×
		ZeroFL [32]	0.05	78.22 ± 0.35	1×	1.9×
		FLASH (ours)	0.05	86.99 ± 0.14	19.5×	19.5×
	non-IID ($\alpha = 1.0$)	ZeroFL [32]	0.1	81.04 ± 0.28	1×	1.6×
		FLASH (ours)	0.1	86.42 ± 0.49	9.8×	9.8×
FEMNIST	non-IID	ZeroFL [32]	0.05	77.16 ± 2.07	1×	17.7×
		FLASH (ours)	0.05	81.18 ± 0.36	14.6×	14.6×

Table 4: Performance of hetero-FLASH where support density set is $d_{set} = [0.1, 0.15, 0.2]$.

Dataset	Data Distribution	Max Client Density	Hetero-FLASH Acc %
MNIST	IID ($\alpha = 1000$)	0.2	98.29 ± 0.05
	non-IID ($\alpha = 1.0$)		98.29 ± 0.09
	non-IID ($\alpha = 0.1$)		97.63 ± 0.22
CIFAR-10	IID ($\alpha = 1000$)	0.2	87.19 ± 0.26
	non-IID ($\alpha = 1.0$)		86.16 ± 0.04
	non-IID ($\alpha = 0.1$)		75.23 ± 1.26
FEMNIST	non-IID	0.2	82.58 ± 0.24

189 However, at comparatively higher density ($d = 0.1$), both can yield models with a lower accuracy
190 difference from the baseline by around 6.46% and 2.82%. FLASH, on the other hand, can maintain
191 **close to the baseline accuracy** at even ultra-low density for all data partitions. *These results clearly*
192 *highlight the efficacy of both sensitivity driven spare learning (as FLASH > PDST) and early mask*
193 *convergence in FL settings.* Moreover, as in FLASH, the clients’ do not need to send the mask at all,
194 *allowing us to yield proportional communication advantage as the model sparsity.*

195 **Comparison with ZeroFL.** Despite leveraging a form of sparse learning [33], ZeroFL required
196 significantly higher up-link/down-link communication cost compared to the target density d . This
197 enables FLASH to gain a significant advantage in communication saving over ZeroFL, particularly
198 for FLASH, as it only asks for the reduced size parameters to be communicated between the server
199 and clients. In particular, we evaluate the communication saving as the ratio of the dense model size
200 and corresponding sparse model size with the tensors represented in compressed sparse row (CSR)
201 format [36]. As depicted in Table 3⁴, FLASH can yield an accuracy improvement of up to 10.1% at a
202 reduced communication cost of up to 10.26× (computed at up-link when both send sparse models).

203 5.2 Experimental Results with Hetero-FLASH

204 Table 4 shows the performance of hetero-FLASH where the clients can have three possible density
205 budgets as defined by the d_{set} . To train on all the density values, we split clients into three groups,
206 each having 40%, 30%, and 30% of total clients, and corresponds to density 0.2, 0.15, and 0.1,
207 respectively. Then, every round, 10% from each group is sampled to participate in training the model.

208 6 Conclusions

209 This paper presented federated lottery-aware sparsity hunting methodologies to yield low parameter
210 density server models with insignificant accuracy drop compared to the dense counterparts. In particu-
211 lar, we demonstrated an efficient sparse learning solution tailored for FL, enabling better computation
212 and communication benefits over existing sparse learning alternatives. We experimentally showed
213 the superiority of our model in yielding up to ~10.1% improved accuracy with ~10.26× fewer
214 communication costs compared to the existing alternatives [32], at similar hyperparameter settings.

215 **Societal impact.** FLASH can efficiently learn low parameter FL models potentially reducing the
216 energy budget thus carbon footprint of edge devices participating in FL.

⁴We understand for FEMNIST, ZeroFL reported significantly higher up-link saving, however, to the best of our understanding it should be similar to their report on other datasets, i.e. ~1.9×.

217 **References**

- 218 [1] Alyazeed Albasyoni, Mher Safaryan, Laurent Condat, and Peter Richtárik. Optimal gradient
219 compression for distributed and federated learning. *arXiv preprint arXiv:2010.03246*, 2020.
- 220 [2] Sameer Bibikar, Haris Vikalo, Zhangyang Wang, and Xiaohan Chen. Federated dynamic
221 sparse training: Computing less, communicating less, yet learning better. *arXiv preprint*
222 *arXiv:2112.09824*, 2021.
- 223 [3] Sebastian Caldas, Sai Meher Karthik Duddu, Peter Wu, Tian Li, Jakub Konečný, H Brendan
224 McMahan, Virginia Smith, and Ameet Talwalkar. Leaf: A benchmark for federated settings.
225 *arXiv preprint arXiv:1812.01097*, 2018.
- 226 [4] Sebastian Caldas, Jakub Konečný, H Brendan McMahan, and Ameet Talwalkar. Expanding
227 the reach of federated learning by reducing client resource requirements. *arXiv preprint*
228 *arXiv:1812.07210*, 2018.
- 229 [5] Tim Dettmers and Luke Zettlemoyer. Sparse networks from scratch: Faster training without
230 losing performance. *arXiv preprint arXiv:1907.04840*, 2019.
- 231 [6] Enmao Diao, Jie Ding, and Vahid Tarokh. Heterofl: Computation and communication efficient
232 federated learning for heterogeneous clients. *arXiv preprint arXiv:2010.01264*, 2020.
- 233 [7] Xiaohan Ding, Xiangxin Zhou, Yuchen Guo, Jungong Han, Ji Liu, et al. Global sparse
234 momentum sgd for pruning very deep neural networks. *Advances in Neural Information*
235 *Processing Systems*, 32, 2019.
- 236 [8] Utku Evci, Trevor Gale, Jacob Menick, Pablo Samuel Castro, and Erich Elsen. Rigging the
237 lottery: Making all tickets winners. In *International Conference on Machine Learning*, pages
238 2943–2952. PMLR, 2020.
- 239 [9] Jonathan Frankle and Michael Carbin. The lottery ticket hypothesis: Finding sparse, trainable
240 neural networks. *arXiv preprint arXiv:1803.03635*, 2018.
- 241 [10] Eduard Gorbunov, Konstantin P Burlachenko, Zhize Li, and Peter Richtárik. Marina: Faster
242 non-convex distributed learning with compression. In *International Conference on Machine*
243 *Learning*, pages 3788–3798. PMLR, 2021.
- 244 [11] Pengchao Han, Shiqiang Wang, and Kin K Leung. Adaptive gradient sparsification for efficient
245 federated learning: An online learning approach. In *2020 IEEE 40th International Conference*
246 *on Distributed Computing Systems (ICDCS)*, pages 300–310. IEEE, 2020.
- 247 [12] Chaoyang He, Murali Annavaram, and Salman Avestimehr. Group knowledge transfer: Feder-
248 ated learning of large cnns at the edge. *Advances in Neural Information Processing Systems*,
249 33:14068–14080, 2020.
- 250 [13] Kaiming He, Xiangyu Zhang, Shaoqing Ren, and Jian Sun. Deep residual learning for image
251 recognition. In *Proceedings of the IEEE conference on computer vision and pattern recognition*,
252 pages 770–778, 2016.
- 253 [14] Yihui He, Ji Lin, Zhijian Liu, Hanrui Wang, Li-Jia Li, and Song Han. Amc: Automl for model
254 compression and acceleration on mobile devices. In *Proceedings of the European conference*
255 *on computer vision (ECCV)*, pages 784–800, 2018.
- 256 [15] Samuel Horvath, Stefanos Laskaridis, Mario Almeida, Ilias Leontiadis, Stylianos Venieris, and
257 Nicholas Lane. Fjord: Fair and accurate federated learning under heterogeneous targets with
258 ordered dropout. *Advances in Neural Information Processing Systems*, 34, 2021.
- 259 [16] Tiansheng Huang, Shiwei Liu, Li Shen, Fengxiang He, Weiwei Lin, and Dacheng Tao. Achiev-
260 ing personalized federated learning with sparse local models. *arXiv preprint arXiv:2201.11380*,
261 2022.
- 262 [17] Rustem Islamov, Xun Qian, and Peter Richtárik. Distributed second order methods with fast
263 rates and compressed communication. In *International Conference on Machine Learning*, pages
264 4617–4628. PMLR, 2021.

- 265 [18] Yuang Jiang, Shiqiang Wang, Victor Valls, Bong Jun Ko, Wei-Han Lee, Kin K Leung, and
266 Leandros Tassiulas. Model pruning enables efficient federated learning on edge devices. *IEEE*
267 *Transactions on Neural Networks and Learning Systems*, 2022.
- 268 [19] Alex Krizhevsky, Geoffrey Hinton, et al. Learning multiple layers of features from tiny images.
269 2009.
- 270 [20] Souvik Kundu, Mahdi Nazemi, Peter A Beerel, and Massoud Pedram. Dnr: A tunable robust
271 pruning framework through dynamic network rewiring of dnns. In *Proceedings of the 26th Asia*
272 *and South Pacific Design Automation Conference*, pages 344–350, 2021.
- 273 [21] Souvik Kundu, Mahdi Nazemi, Massoud Pedram, Keith M Chugg, and Peter A Beerel. Pre-
274 defined sparsity for low-complexity convolutional neural networks. *IEEE Transactions on*
275 *Computers*, 69(7):1045–1058, 2020.
- 276 [22] Yann LeCun and Corinna Cortes. MNIST handwritten digit database. 2010.
- 277 [23] Ang Li, Jingwei Sun, Binghui Wang, Lin Duan, Sicheng Li, Yiran Chen, and Hai Li. Lotteryfl:
278 Personalized and communication-efficient federated learning with lottery ticket hypothesis on
279 non-iid datasets. *arXiv preprint arXiv:2008.03371*, 2020.
- 280 [24] Ang Li, Jingwei Sun, Xiao Zeng, Mi Zhang, Hai Li, and Yiran Chen. Fedmask: Joint computa-
281 tion and communication-efficient personalized federated learning via heterogeneous masking.
282 In *Proceedings of the 19th ACM Conference on Embedded Networked Sensor Systems*, pages
283 42–55, 2021.
- 284 [25] Tian Li, Anit Kumar Sahu, Manzil Zaheer, Maziar Sanjabi, Ameet Talwalkar, and Virginia
285 Smith. Federated optimization in heterogeneous networks. *Proceedings of Machine Learning*
286 *and Systems*, 2:429–450, 2020.
- 287 [26] Xiang Li, Kaixuan Huang, Wenhao Yang, Shusen Wang, and Zhihua Zhang. On the convergence
288 of fedavg on non-iid data. *arXiv preprint arXiv:1907.02189*, 2019.
- 289 [27] Tao Lin, Lingjing Kong, Sebastian U Stich, and Martin Jaggi. Ensemble distillation for robust
290 model fusion in federated learning. *Advances in Neural Information Processing Systems*,
291 33:2351–2363, 2020.
- 292 [28] Shiwei Liu, Decebal Constantin Mocanu, Amarsagar Reddy Ramapuram Matavalam, Yulong
293 Pei, and Mykola Pechenizkiy. Sparse evolutionary deep learning with over one million artificial
294 neurons on commodity hardware. *Neural Computing and Applications*, 33(7):2589–2604, 2021.
- 295 [29] Xiaolong Ma, Sheng Lin, Shaokai Ye, Zhezhi He, Linfeng Zhang, Geng Yuan, Sia Huat
296 Tan, Zhengang Li, Deliang Fan, Xuehai Qian, et al. Non-structured dnn weight pruning—is it
297 beneficial in any platform? *IEEE Transactions on Neural Networks and Learning Systems*,
298 2021.
- 299 [30] Brendan McMahan, Eider Moore, Daniel Ramage, Seth Hampson, and Blaise Aguera y Arcas.
300 Communication-efficient learning of deep networks from decentralized data. In *Artificial*
301 *intelligence and statistics*, pages 1273–1282. PMLR, 2017.
- 302 [31] Decebal Constantin Mocanu, Elena Mocanu, Peter Stone, Phuong H Nguyen, Madeleine
303 Gibescu, and Antonio Liotta. Scalable training of artificial neural networks with adaptive sparse
304 connectivity inspired by network science. *Nature communications*, 9(1):1–12, 2018.
- 305 [32] Xinchu Qiu, Javier Fernandez-Marques, Pedro PB Gusmao, Yan Gao, Titouan Parcollet, and
306 Nicholas Donald Lane. Zeroff: Efficient on-device training for federated learning with local
307 sparsity. In *International Conference on Learning Representations*, 2021.
- 308 [33] Md Aamir Raihan and Tor Aamodt. Sparse weight activation training. *Advances in Neural*
309 *Information Processing Systems*, 33:15625–15638, 2020.
- 310 [34] Sashank Reddi, Zachary Charles, Manzil Zaheer, Zachary Garrett, Keith Rush, Jakub Konečný,
311 Sanjiv Kumar, and H Brendan McMahan. Adaptive federated optimization. *arXiv preprint*
312 *arXiv:2003.00295*, 2020.

- 313 [35] Ao Ren, Tianyun Zhang, Shaokai Ye, Jiayu Li, Wenyao Xu, Xuehai Qian, Xue Lin, and Yanzhi
314 Wang. Admm-nn: An algorithm-hardware co-design framework of dnns using alternating
315 direction methods of multipliers. In *Proceedings of the Twenty-Fourth International Conference*
316 *on Architectural Support for Programming Languages and Operating Systems*, pages 925–938,
317 2019.
- 318 [36] William F Tinney and John W Walker. Direct solutions of sparse network equations by optimally
319 ordered triangular factorization. *Proceedings of the IEEE*, 55(11):1801–1809, 1967.
- 320 [37] Dezhong Yao, Wanning Pan, Yao Wan, Hai Jin, and Lichao Sun. Fedhm: Efficient federated
321 learning for heterogeneous models via low-rank factorization. *arXiv preprint arXiv:2111.14655*,
322 2021.
- 323 [38] Haoran You, Chaojian Li, Pengfei Xu, Yonggan Fu, Yue Wang, Xiaohan Chen, Richard G
324 Baraniuk, Zhangyang Wang, and Yingyan Lin. Drawing early-bird tickets: Towards more
325 efficient training of deep networks. *arXiv preprint arXiv:1909.11957*, 2019.
- 326 [39] Tianyun Zhang, Shaokai Ye, Kaiqi Zhang, Jian Tang, Wujie Wen, Makan Fardad, and Yanzhi
327 Wang. A systematic dnn weight pruning framework using alternating direction method of
328 multipliers. In *Proceedings of the European Conference on Computer Vision (ECCV)*, pages
329 184–199, 2018.
- 330 [40] Tuo Zhang, Lei Gao, Chaoyang He, Mi Zhang, Bhaskar Krishnamachari, and Salman Aves-
331 timehr. Federated learning for internet of things: Applications, challenges, and opportunities.
332 *arXiv preprint arXiv:2111.07494*, 2021.
- 333 [41] Yuchen Zhang, John Duchi, Michael I Jordan, and Martin J Wainwright. Information-theoretic
334 lower bounds for distributed statistical estimation with communication constraints. In C.J.
335 Burges, L. Bottou, M. Welling, Z. Ghahramani, and K.Q. Weinberger, editors, *Advances in*
336 *Neural Information Processing Systems*, volume 26. Curran Associates, Inc., 2013.
- 337 [42] Zhuangdi Zhu, Junyuan Hong, and Jiayu Zhou. Data-free knowledge distillation for het-
338 erogeneous federated learning. In *International Conference on Machine Learning*, pages
339 12878–12889. PMLR, 2021.

340 Checklist

- 341 1. For all authors...
- 342 (a) Do the main claims made in the abstract and introduction accurately reflect the paper’s
343 contributions and scope? [Yes]
- 344 (b) Did you describe the limitations of your work? [Yes]
- 345 (c) Did you discuss any potential negative societal impacts of your work? [N/A]
- 346 (d) Have you read the ethics review guidelines and ensured that your paper conforms to
347 them? [Yes]
- 348 2. If you are including theoretical results...
- 349 (a) Did you state the full set of assumptions of all theoretical results? [N/A]
- 350 (b) Did you include complete proofs of all theoretical results? [N/A]
- 351 3. If you ran experiments...
- 352 (a) Did you include the code, data, and instructions needed to reproduce the main experi-
353 mental results (either in the supplemental material or as a URL)? [Yes]
- 354 (b) Did you specify all the training details (e.g., data splits, hyperparameters, how they
355 were chosen)? [Yes]
- 356 (c) Did you report error bars (e.g., with respect to the random seed after running experi-
357 ments multiple times)? [Yes]
- 358 (d) Did you include the total amount of compute and the type of resources used (e.g., type
359 of GPUs, internal cluster, or cloud provider)? [Yes]
- 360 4. If you are using existing assets (e.g., code, data, models) or curating/releasing new assets...
- 361 (a) If your work uses existing assets, did you cite the creators? [Yes]

- 362 (b) Did you mention the license of the assets? [N/A]
 363 (c) Did you include any new assets either in the supplemental material or as a URL? [Yes]
 364 (d) Did you discuss whether and how consent was obtained from people whose data you're
 365 using/curating? [N/A]
 366 (e) Did you discuss whether the data you are using/curating contains personally identifiable
 367 information or offensive content? [N/A]
 368 5. If you used crowdsourcing or conducted research with human subjects...
- 369 (a) Did you include the full text of instructions given to participants and screenshots, if
 370 applicable? [N/A]
 371 (b) Did you describe any potential participant risks, with links to Institutional Review
 372 Board (IRB) approvals, if applicable? [N/A]
 373 (c) Did you include the estimated hourly wage paid to participants and the total amount
 374 spent on participant compensation? [N/A]

375 7 Supplementary

376 7.1 Model Architectures

377 Table 5 shows the model architectures used for MNIST and FEMNIST datasets. For CIFAR-10 we
 used ResNet18 [13] with the first CONV layer kernel size as 3×3 instead of original 7×7 .

Table 5: Architecture used for MNIST and FEMNIST datasets

MNIST	FEMNIST
$\text{CONV}5 \times 5 (C_o = 10)$	$\text{CONV}5 \times 5 (C_o = 32)$
max_pool	max_pool
$\text{CONV}5 \times 5 (C_o = 20)$	$\text{CONV}5 \times 5 (C_o = 64)$
max_pool	max_pool
$\text{FC}(5120, 50)$	$\text{FC}(3136, 2048)$
$\text{FC}(50, 10)$	$\text{FC}(2028, 62)$

378

379 7.2 Hetero-FLASH Algorithm

380 Algorithm 2 details the training algorithm in hetero-FLASH.

Algorithm 2: Hetero-FLASH Training.

Data: Training rounds T , local epochs E , client set $[[\mathcal{C}_{N_1}], \dots, [\mathcal{C}_{N_M}]]$, clients per rounds c_r , target density set $d_{set} = [d_1, \dots, d_M]$, sensitivity warm-up epochs E_d , density warm up client count c_d , initial value of freeze masks $m_{freeze} = 0$ and aggregation type t_{aggr} .

```
1  $\mathcal{M}^{init} \leftarrow \text{createRandomMask}()$ 
2  $\Theta^{init} \leftarrow \text{initMaskedWeight}(\mathcal{M}^{init})$ 
3 serverExecute:
4 Randomly sample  $c_d$  clients  $[\mathcal{C}_d] \subset [\mathcal{C}_{N_M}]$ 
5 for each client  $c \in [\mathcal{C}_d]$  in parallel do
6    $\Theta_c \leftarrow \text{clientExecute}(\Theta^{init}, E_d, 0)$ 
7    $\mathcal{S}_c \leftarrow \text{computeSensitivity}(\Theta_c)$ 
8 end
9  $\mathcal{M}^0 \leftarrow \text{initMask}([\mathcal{S}_c], d_{set})$ 
10  $\Theta^0 \leftarrow \text{initMaskedWeight}(\mathcal{M}^0)$ 
11  $m_{freeze} \leftarrow 1$ 
12 for each round  $t \leftarrow 1$  to  $T$  do
13   Randomly sample  $c_r$  clients  $[\mathcal{C}_r] \subset [\mathcal{C}_N]$ 
14   for each client  $c \in [\mathcal{C}_r]$  in parallel do
15      $\Theta_c^{t-1} \leftarrow \text{applyClientMask}(\Theta^{t-1}, c)$ 
16      $\Theta_c^t \leftarrow \text{clientExecute}(\Theta_c^{t-1}, E, m_{freeze})$ 
17   end
18    $\Theta^t \leftarrow \text{aggrParam}([\Theta_c^t], t_{aggr})$ 
19 end
20 clientExecute $(\Theta_c, E, m_{freeze})$  :
21  $\Theta_{c^0} \leftarrow \Theta_c$ 
22 for local epoch  $i \leftarrow 1$  to  $E$  do
23    $\Theta_{c^i} \leftarrow \text{doSparseLearning}(\Theta_{c^{i-1}}, m_{c^{freeze}})$ 
24 end
25 return  $\Theta_{c^E}$ 
```
